Controllable electrostatic surface guide for cold molecules with a single charged wire

Zhenxing Gu, Chaoxiu Guo, Shunyong Hou, Shengqiang Li, Lianzhong Deng, and Jianping Yin*
State Key Laboratory of Precision Spectroscopy, Department of Physics, East China Normal University, Shanghai, 200062, People's Republic of China

(Received 5 February 2013; published 3 May 2013)

We demonstrate a controllable highly efficient electrostatic surface guide for ND_3 molecules in the weak-field-seeking states on a ceramic substrate over a distance of 840 mm, and study the dependences of the relative molecule number (or the overall transmission efficiency) of our single-wire guide and the guiding-center positions on the guiding voltages, both experimentally and theoretically. Our study shows that the guiding-center position and the number of the guided molecules can be easily controlled by adjusting the guiding voltages, and find that an overall transmission efficiency of higher than 50% in a single quantum state can be obtained. Our experimental results are consistent with ones of Monte Carlo simulations. Also, we discuss the transverse velocity filtering effect and the acceptance of the guided molecules in four-dimensional phase space. Both the transmission efficiency and the acceptance in two-dimensional position space are higher than that in our previous two-wire guide [Y. Xia, Y. Yin, H. Chen, L. Deng, and J. Yin, Phys. Rev. Lett. **100**, 043003 (2008)].

DOI: 10.1103/PhysRevA.87.053401 PACS number(s): 37.10.Pq, 37.10.Mn, 03.75.Be, 37.10.Gh

I. INTRODUCTION

Cold and ultracold molecules have plenty of applications in the fields of high-resolution spectroscopy [1,2], quantum control [3], cold collisions [4–6], cold chemistry [7], and quantum information science [8], etc. In order to carry out the above applied studies of cold molecules, scientists have developed various molecular guiding techniques in recent years. Among the schemes that have been proposed and demonstrated are a Keppler-type electrostatic guide for polar molecules in the strong-field-seeking (SFS) states [9,10], and a curved electrostatic quadrupole [11–13] or hexapole [14,15] guide for cold polar molecules in the weak-field-seeking (WFS) states. In 2005, we proposed an electrostatic surface guiding scheme to guide polar molecules in the WFS states using a pair of parallel charged wires and a grounded metal plate [16]. In 2008, we demonstrated this two-wire guiding scheme experimentally [17]. In these guiding schemes, however, the position of the guiding center of cold molecules and its motion cannot be easily controlled by changing the guiding voltage. In particular, the above Keppler-type and quadrupole or hexapole guiding schemes [9–15] cannot be used to realize the electrostatic surface guide of cold molecules on a chip, while the surface guiding efficiency of our two-wire guiding scheme [16,17] for cold (ND_3, D_2O, etc.) molecules is not usually very high, and its acceptance in position space is not large. As an alternative guide scheme, we use a single charged wire on a ceramic substrate and a pair of parallel metal plates in this work. In this scheme, the position of the guiding center of cold molecules and its guided molecular number can be easily controlled by changing the guiding voltages, and its acceptance in position space is large so as to obtain a high loading efficiency. It is clear that this scheme reduces the elegance and practicality of a molecular chip as compared with our two-wire guide [16,17]. However, to obtain a higher loading efficiency and realize the controllability of the guided cold molecules, the sacrifice of the elegance is also worthwhile, and the issues of practicality of the molecular chip (i.e., the laser manipulation, controlling, and probe of the guided cold molecules) can be solved basically by using a transparent electrode to replace our upper metal plate. In this paper, we demonstrate a controllable, highly efficient electrostatic surface guiding scheme, and study the dependences of the molecular transmission efficiencies on the guiding voltages. Also, we study the dependence of the relative molecule number in the guide on the guiding distance, and briefly discuss the transverse velocity filtering effect and the acceptance of the guided cold molecules in four-dimensional (4D) phase space compared to our previous two-wire scheme [16,17]. Finally, we discuss some potential applications of our guiding scheme in the preparation of cold molecules and integrated molecule optics, etc.

II. EXPERIMENTAL SETUP

Our experimental setup is similar to one reported earlier [18] with the difference that the charged Y-shaped wire is replaced by a straight charged wire, as shown in Fig. 1. The length of the straight stainless wire, with a diameter of 2 mm and a high voltage U_1, is shortened to 840 mm. The voltage applied to the upper metal plate is U_2, while the lower metal plate is grounded. The dielectric strength of the ceramic substrate is greater than 60 kV/cm. We calculate the electric field distribution above the charged wire and find that there is a hollow electrostatic field distribution [see Figs. 1(a) and 2], which can be used to guide cold polar molecules in the WFS states.

The experimental setup is composed of two differentially pumped vacuum chambers. One is the source chamber for generating a supersonic molecular beam, and the other is the guiding chamber containing a molecular guiding device and a detecting system. The limited and operating vacuum pressures in the source chamber are typically 1.1×10^{-8} and 2.4×10^{-4} Pa, respectively, while the limited and operating vacuum pressures in the guiding chamber are 1.0×10^{-7} and 6.5×10^{-7} Pa. To ionize and detect molecular signals, we use a homemade time-of-flight mass spectrometer, which is the same as the one in Ref. [18]. A pulsed supersonic molecular beam is formed by adiabatically expanding a gaseous mixture

*Corresponding author: jpyin@phy.ecnu.edu.cn

 ©2013 American Physical Society

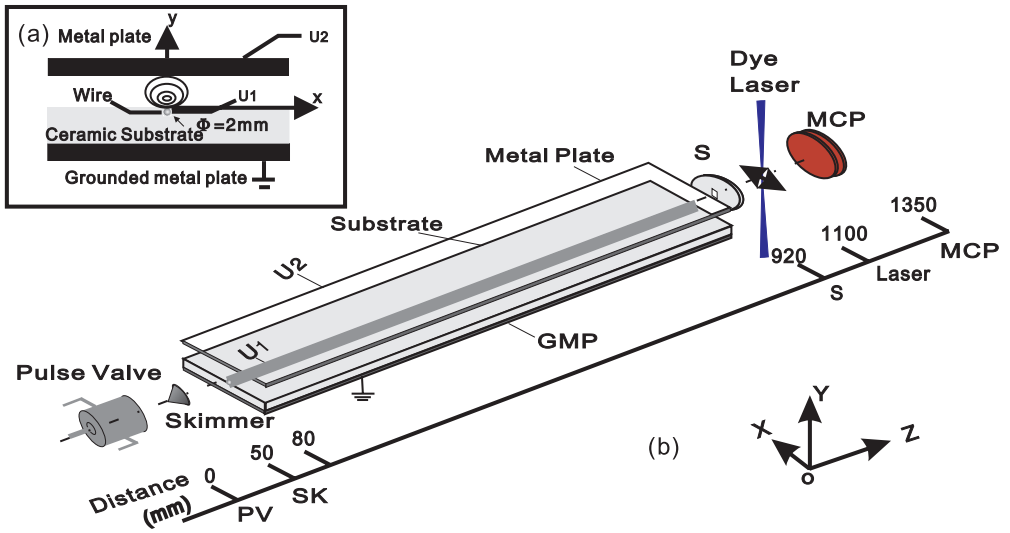

FIG. 1. (Color online) (a) Cross-sectional view of electrostatic guiding scheme composed of a single charged straight wire and a pair of metal plates, including the contours profile of electric field above the wire; (b) experimental setup and the locations of each element in front of the nozzle. PV, SK, S, and MCP stand for pulse valve, skimmer, sampling hole, and microchannel plate.

consisting of 5.0% ND_3 and the carrier gas xenon through a solenoid valve into vacuum with a source pressure of 2.5 atm and a source temperature of $-40\,^{\circ}$C, which is obtained by a temperature-controllable liquid nitrogen cooling system.

After passing through a skimmer with a diameter of 1 mm, the supersonic molecular beam enters the guiding chamber and is loaded into the electrostatic guiding tube. The output molecular beam goes through a 4 mm $\times$ 6 mm sampling hole and then flies freely for a short distance of 180 mm, after which the molecules are ionized by the dye laser and detected by using resonant enhanced multiphoton $(2+1)$ ionization (REMPI) spectroscopy. The ion signals are amplified by two microchannel plates (MCP), and the amplified signals are collected and averaged over 128 shots on an oscilloscope (HP 54616C, 500 MHz) connected to a personal computer for signal storage and data processing.

III. EXPERIMENTAL AND SIMULATED RESULTS

To check the controllability of cold molecules in our guiding scheme, we theoretically study the dependence of the guiding-center position y_0 on the guiding voltage U_1 when U_2 is fixed, and the results are shown in Fig. 3. The dashed line shows that the guiding-center position y_0 grows exponentially with the increase of the guiding voltage U_1 for $U_2 = 16$ kV. It indicates that we can easily control the guiding-center position by adjusting the voltage U_1 for a fixed U_2, which brings

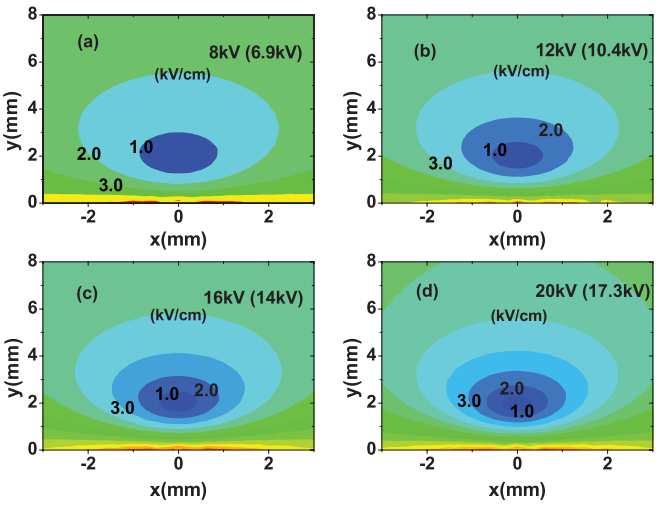

FIG. 2. (Color online) Contours of the electric field magnitude in the xy plane for different voltage pairs U_2 (U_1). (a)–(d), show contours for U_2 (U_1) = 8 kV (6.9 kV), 12 kV (10.4 kV), 16 kV (14 kV), and 20 kV (17.3 kV), respectively.

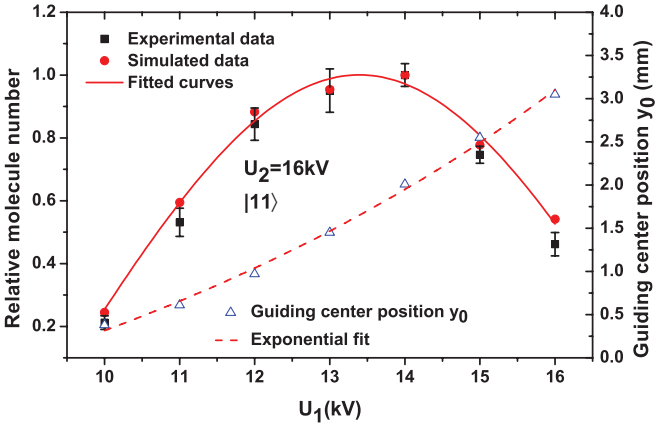

FIG. 3. (Color online) Dependences of the position of the molecular guiding center and the normalized guiding molecular number on the guiding voltage U_1 for $U_2 = 16$ kV. Squares with an error bar are the experimental data, while circles are Monte Carlo simulation data, corresponding to the left y axis. Triangles are the calculated guiding-center positions, corresponding to the right y axis. Solid and dotted lines are the fitted curves.

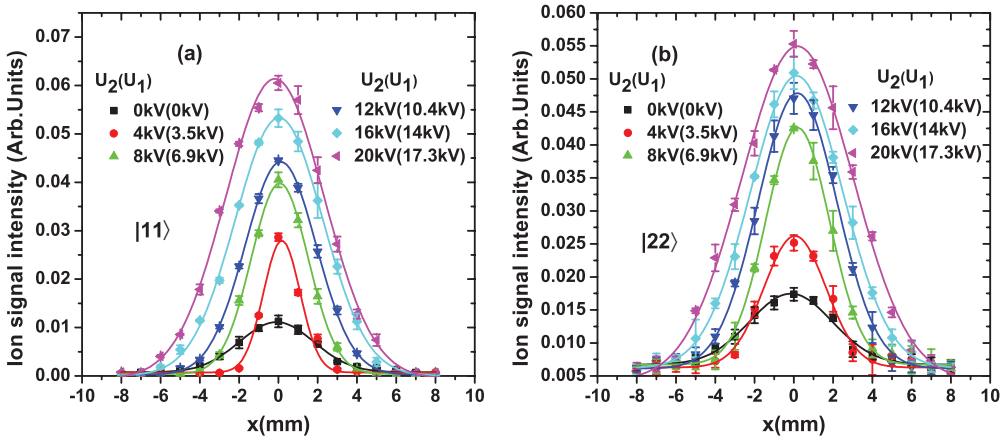

FIG. 4. (Color online) Relative ion signal intensity of the guided ND_3 molecules versus the transverse position for different guiding voltage pairs U_2 (U_1) in (a) the $|11\rangle$ state, and (b) the $|22\rangle$ state. Various symbols with error bars are the experimental data, and the solid lines are fitted Gaussian profile.

convenience to our experimental operation. Once the guiding device is fixed in the vacuum chamber, the injecting coupling between the incident molecular beam and the electrostatic guiding tube is one of the most important constraints governing the guided molecule number. With the advantage of the controllability of the guiding-center position in our scheme, we can get good injecting coupling by adjusting U_1, and obtain the largest guided molecule number corresponding to an optimal U_1.

For a quantitative description, we calculate the electric field distribution above the guiding wire, and perform Monte Carlo simulations for the dynamics of the guided ND_3 molecules. Our simulation method and its details are similar to those in Ref. [19], and in this paper, the Stark shift of ND_3 can be described by [20]

$$W_{\text{Stark}}(r) = \pm\sqrt{\left(-\frac{\mu_e E(r) K M}{J(J+1)}\right)^2 + \left(\frac{W_{\text{inv}}}{2}\right)^2} + \frac{W_{\text{inv}}}{2},$$

where W_{Stark}, μ_e (1.48 D [21]), $E(r)$, and W_{inv} (1.7 GHz) are the Stark shift, the electric dipole moment, the electrostatic field distribution, and the inversion splitting, respectively.

The simulated ND_3 molecular beam is centered around 307 m/s with a velocity spread of 60 m/s in the longitudinal direction, and has a velocity spread of 15 m/s centered around zero in the transverse direction, while the position spreads in the x and y directions are both set to be 1 mm. The simulated results are shown in Fig. 3 when $U_2 = 16$ kV. With the increase of the voltage U_1 from 10 to 16 kV, the normalized guided molecular number is first increased from about 0.2 to 1, and then reduced to 0.45 in the $|JK\rangle = |11\rangle$ state. We measure the transverse distribution of the guided ND_3 molecules experimentally under the same conditions, and find that with the increase of the guiding voltage U_1, the relative signal intensity is also first increased and then reduced, and all the transverse profiles of the guided ND_3 beam are Gaussian ones. Because the integrated area of each transverse profile is proportional to the flux or number of the guided molecules, we can obtain the experimental dependence of the normalized molecular number on the guiding voltage U_1 (black squares in Fig. 3), which is in good agreement with the Monte Carlo simulation. This shows that there is an optimal value of U_1 (about 14 kV) to obtain the largest guided molecular number. It is clear from Fig. 3 that the number of the guided cold molecules as well as their motion can be controlled conveniently by changing the guiding voltage U_1.

We can find from Fig. 3 that when $U_1 = 14$ kV and $U_2 = 16$ kV, the guiding-center position y_0 is equal to 2 mm, and it is also the center position of the incident supersonic molecular beam in the y direction. With the same method, we obtain series voltage pairs U_2 (U_1) = 4 kV (3.5 kV), 8 kV (6.9 kV), 12 kV (10.4 kV), 16 kV (14 kV), and 20 kV (17.3 kV), and the corresponding electric field contours of the last four pairs of guiding voltages are shown in Fig. 2. It shows that the transverse trapping depth increases with the growth of the guiding voltages U_2 (U_1), while all guiding-center positions are located almost at the same height (~2 mm) for all of the voltage pairs.

Afterwards, we measure the transverse distribution of the guided molecular beam in both the $|11\rangle$ and $|22\rangle$ states under the above voltage pairs experimentally, and the results (see Fig. 4) show that the higher the guiding voltages U_2 (U_1) are, the higher the relative signal intensity is. Since the integrated area under each transverse profile is proportional to the number of the guided molecules, the relative transmission efficiency can be defined as the ratio of the integrated area at each voltage pair U_2 (U_1) to the maximum integrated area at U_2 (U_1) = 20 kV (17.3 kV), after subtracting from all integrated areas the background integrated area measured at $U_1 = U_2 = 0$. Figure 5 shows the dependences of the relative transmission efficiencies in both the $|11\rangle$ and $|22\rangle$ states on the guiding voltages U_2 (U_1). It is clear that the higher the guiding voltages are, the higher the relative transmission efficiency will be, and our experimental results divided by about 1.9 are in good agreement with the simulated ones. The simulated transmission efficiency in the $|11\rangle$ state is about 0.53, which multiplied by 1.9 is about equal to our measured relative efficiency when U_2 (U_1) = 20 kV (17.3 kV). We also can see from Fig. 5 that when U_2 (U_1) = 4 kV (3.5 kV), the transmission efficiency for ND_3 molecules in the $|11\rangle$ state is slightly lower than one in the $|22\rangle$ state,

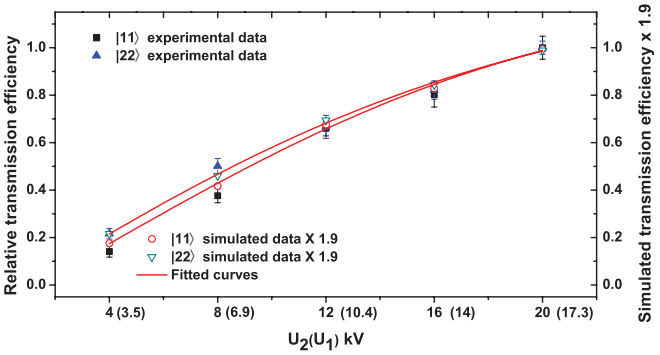

FIG. 5. (Color online) Dependences of the transmission efficiency of the guided cold molecules on the guiding voltages U_2 (U_1) in both the $|11\rangle$ and $|22\rangle$ states. Here the label 4 (3.5) in the transverse coordinate means $U_2 = 4$ kV and $U_1 = 3.5$ kV, and similarly for the others. Various symbols with error bars are the experimental data, and the solid lines are the fitted curves.

and with the increase of the guiding voltages, the difference between the transmission efficiencies in the two WFS states becomes smaller, and when U_2 (U_1) = 20 kV (17.3 kV), the transmission efficiency for ND_3 in the $|11\rangle$ state reaches to 0.53, which is about equal to that of the $|22\rangle$ state.

According to the above discussion, we know that the transmission efficiency of our single-wire guide can be increased by simply applying higher voltages. Theoretically, the upper limit of the voltages applied to the electrodes only depends on the dielectric strength and the thickness of the ceramic substrate. For the given dielectric strength of greater than 60 kV/cm and a thickness of 14 mm, we can estimate that U_1 can be as large as 84 kV, and then the transmission efficiency can be much larger. However, the upper limit to voltages applied to the electrodes in our experiment depends on both the onset of discharges between the electrodes and charge leakage between the electrode and the insulated substrate, which occurs at less than 21 kV in our experiment. For safety, the guiding voltage used in our experiment is limited to 20 kV.

IV. ANALYSIS AND DISCUSSION

To better understand the loading and guiding processes of cold molecules, we perform Monte Carlo simulations and discuss the transverse velocity filtering effect in the straight guide and the acceptance of the guided cold molecules in 4D phase space. In our simulation, we still take the voltage pairs U_2 (U_1) = 8 kV (6.9 kV), 12 kV (10.4 kV), 16 kV (14 kV), and 20 kV (17.3 kV) to study the dependence of the relative guided molecular number on the guiding distance L. The simulated results are shown as the square data points in Figs. 6(a)–6(d), respectively. For each voltage pair, the relative molecule number first decreases with increasing guiding distance, and then remains constant after a certain position. We define this position as the stable guiding distance. This effect occurs because the transverse temperature of the incident molecular beam is far higher than the transverse potential-well depth of our electrostatic guide, so many hot molecules with higher transverse kinetic energies will be gradually lost from the transverse direction during the molecular loading and guiding process, which can be regarded as a transverse velocity filtering

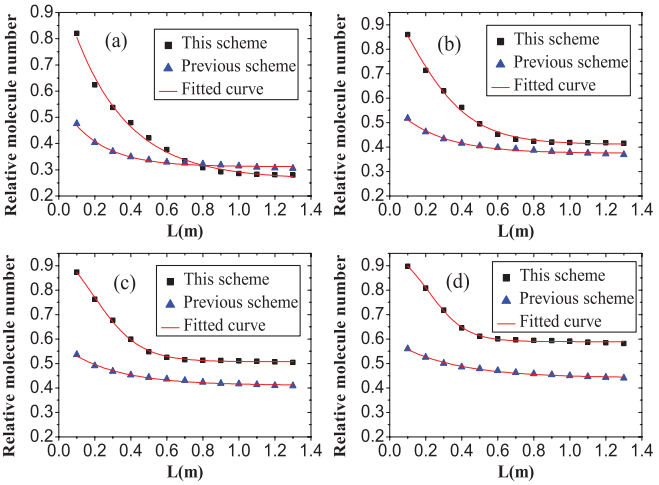

FIG. 6. (Color online) Dependence of the relative molecular number around the guide on the guiding distances when U_2 (U_{wire}) is (a) 8 kV (6.9 kV), (b) 12 kV (10.4 kV), (c) 16 kV (14 kV), and (d) 20 kV (17.3 kV) for the present guide, and when U_{wire} is (a) 6.9 kV, (b) 10.4 kV, (c) 14 kV, and (d) 17.3 kV for the two-wire scheme.

effect on the guided molecular beam. When all hot molecules with kinetic energies higher than the Stark potential energy are lost after a certain guiding distance, the guided molecular number will never change again. It is also found that with the increase of the guiding voltages, the stable guiding distance will occur earlier, which is because the higher the guiding voltages are, the deeper the transverse potential well is; thus fewer molecules are lost, and the transverse filtering process finishes sooner.

To compare with our previous surface guiding scheme (i.e., the two-wire scheme) [16], we also perform the simulations for the two-wire scheme with the same input parameters of the initial molecular beam. The voltages applied to the two wires are equal to the voltage applied to the single wire in our present scheme. They are 6.9, 10.4, 14, and 17.3 kV, and the simulated results with triangles are shown in Figs. 6(a)–6(d), respectively. It is clear from Fig. 6 that the guided relative molecule number in our single-wire scheme is slightly smaller than that in the two-wire scheme at a lower guiding voltage (6.9 kV), but with the increase of the guiding voltage, the number of guided molecules in our single-wire scheme grows significantly, and exceeds that in our previous two-wire scheme.

Usually, the capability of a guide system is parametrized by the ranges of the transverse positions and velocities of the guided particles that can be transported without any beam loss, and this parameter is called the acceptance of the guide. Figure 7 shows the distributions of the guided cold molecules in the $|11\rangle$ state in the two-dimensional (2D) (x, y) position space [see Figs. 7(a) and 7(b)] and 2D (v_x, v_y) velocity space [see Figs. 7(c) and 7(d)] after being guided above the single charged wire for 840 mm. Here Figs. 7(a) and 7(c) are the simulated results when U_2 (U_1) = 8 kV (6.9 kV), while Figs. 7(b) and 7(d) are the results when U_2 (U_1) = 20 kV (17.3 kV). Most cold molecules with lower kinetic energies are accepted near the minimum of the effective guiding potential well, and some hot molecules with higher kinetic energies will move outside the acceptance region and will not reach

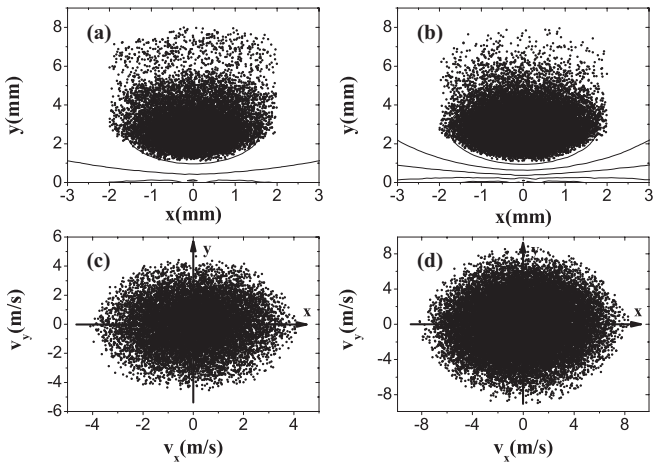

FIG. 7. Distributions of cold ND_3 molecules in the $|11\rangle$ state in 2D position space [see (a) and (b)] and 2D velocity space [see (c) and (d)] when (a), (c) U_2 (U_1) = 8 kV (6.9 kV) and (b), (d) 20 kV (17.3 kV).

the end of the guide if the guiding distance is long enough. It can be seen from Fig. 7 that many more molecules are accepted in the guiding region when U_2 (U_1) = 20 kV (17.3 kV), relative to when U_2 (U_1) = 8 kV (6.9 kV). Although the acceptance of cold molecules in 2D position space when U_2 (U_1) = 20 kV (17.3 kV) is slightly smaller than that when U_2 (U_1) = 8 kV (6.9 kV), the velocity distribution of cold molecules for U_2 (U_1) = 20 kV (17.3 kV) is significantly broader than for U_2 (U_1) = 8 kV (6.9 kV). This indicates that the transmission efficiency of guided molecules when U_2 (U_1) = 20 kV (17.3 kV) is larger than when U_2 (U_1) = 8 kV (6.9 kV), which is consistent with the results discussed in Sec. III.

To characterize the acceptance of our guide quantitatively, we examine the 2D statistics of the simulated guided molecular distributions. In our simulation, we properly extend the guiding distance to a key value (i.e., the stable guiding distance) to ensure the number of guided molecules is a constant for voltage pairs U_2 (U_1) = 4 kV (3.5 kV), 8 kV (6.9 kV), 12 kV (10.4 kV), 16 kV (14 kV), and 20 kV (17.3 kV). Figure 8(a) shows that with the growth of the guiding voltages, the acceptance of cold molecules in 2D position space decreases slowly, while the acceptance in 2D velocity space increases greatly [see Fig. 8(b)].

In Fig. 8, we also show the acceptances of the two-wire scheme [16,17], where U_{wire}, the voltages applied to the two-wire electrodes, are 3.5, 6.9, 10.4, 14, and 17.3, respectively. It is clear from Fig. 8 that the acceptance of the two-wire scheme in 2D velocity space is larger than one of our single-wire one by about a factor of 3. However, the acceptance of the two-wire scheme in 2D position space is far smaller than that of our single-wire scheme, by about a factor of 8. Taking into account these two factors and the current supersonic beam parameters, the transmission efficiency of the present single-wire guide will be higher than that of the two-wire scheme [17] for the upper ranges of the guiding voltages, which is consistent with the simulated results in Fig. 6.

From the above experimental results, we can see that our proposed controllable high-efficiency electrostatic surface guiding scheme has some important applications. First of all, our surface guiding scheme can be used to form various integrated molecule-optical devices, such as a Y-shaped electrostatic molecular-beam splitter (EMBS) [18], a molecular interferometer, an electrostatic surface velocity filter (ESVF), an electrostatic surface storage ring (ESSR) [22], and an electrostatic surface Stark decelerator (ESSD) on a chip. In addition, these molecule-optical devices can be used to prepare cold molecules, to perform precise measurements and study cold collisions and cold chemistry [23], and even to study integrated molecule optics on a chip [24,25], possibly including research on nanometer-scale molecular deposition [26], quantum computing and information processing, and so on.

V. CONCLUSIONS

In this paper, we have demonstrated a controllable, highly efficient electrostatic surface guiding scheme for a supersonic

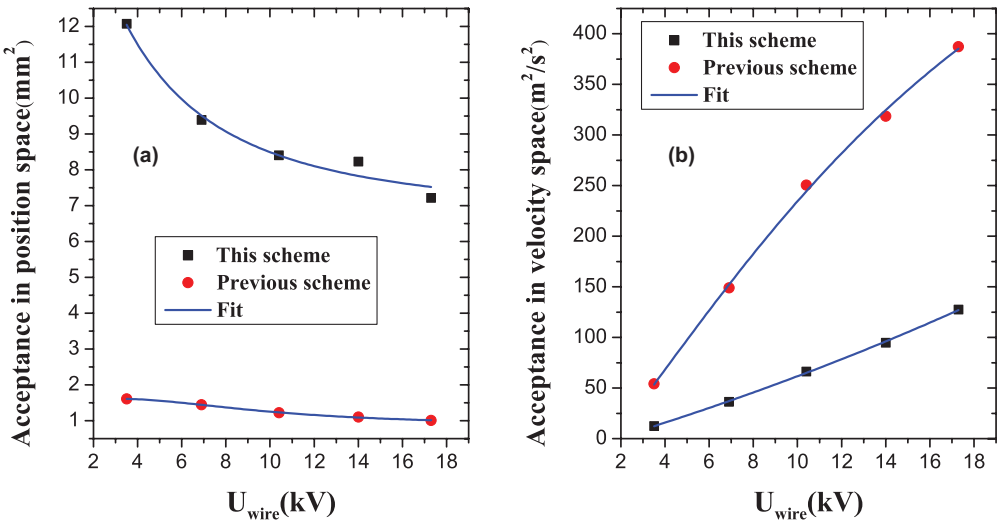

FIG. 8. (Color online) Dependences of the acceptance of cold molecules in both (a) 2D position space and (b) 2D velocity space (i.e., 2D momentum space) on the guiding voltage U_{wire}. Here U_{wire} means the voltage applied to the wire.

ND_3 molecular beam, and studied the dependences of the guiding-center position and the relative molecular number on the guiding voltages, both experimentally and theoretically. We have also briefly discussed the transverse velocity filtering effect and the acceptance of the guided cold molecules in 4D phase space of our guide, and compare the guiding properties of our single-wire scheme to a previous two-wire scheme. Our study shows that (1) the guiding-center position and the relative molecule number can be easily controlled by changing the guiding voltages. (2) When $U_1 = 17.3$ kV, and $U_2 = 20$ kV, a supersonic ND_3 molecular beam in the $|JK\rangle = |11\rangle$ state ($|JK\rangle = |22\rangle$ state) can be efficiently guided in our single charged wire scheme, and a transmission efficiency of higher than 50% can be obtained. (3) With the increase of guiding voltages, the acceptance of the guided cold molecules in 2D position space will be slowly reduced, while the acceptance in 2D velocity space will be rapidly increased. In addition, compared with our previous two-wire scheme [17], the guiding-center position of our present single-wire scheme can be easily adjusted by controlling the guiding voltages, facilitating alignment in the vacuum chamber, and our single-wire scheme has a higher transmission efficiency than our previous two-wire scheme when the guiding voltage U_{wire} is higher than 10.4 kV. Finally, our proposed highly efficient guiding scheme can be used to form various molecule-optical elements [18,22], and has some important applications in cold molecule physics and cold chemistry [23], integrated molecule optics and molecule chip [24,25], precise measurement, and quantum information science, etc.

ACKNOWLEDGMENTS

This work is supported by the National Nature Science Foundation of China under Grants No. 10674047, No. 10804031, No. 10904037, No. 10974055, No. 11034002, No. 61205198, and No. 11274114; the National Key Basic Research and Development Program of China under Grants No. 2006CB921604 and No. 2011CB921602; the Basic Key Program of Shanghai Municipality under Grant No. 07JC14017; and the Shanghai Leading Academic Discipline Project under Grant No. B408.

[1] J. T. Kim, D. Wang, E. E. Eyler, P. L. Gould, and W. C. Stwalley, New J. Phys. **11**, 055020 (2009).
[2] J. van Veldhoven, J. Küpper, H. L. Bethlem, B. Sartakov, A. J. A. van Roij, and G. Meijer, Eur. Phys. J. D **31**, 337 (2004).
[3] E. A. Shapiro, A. Pe'er, J. Ye, and M. Shapiro, Phys. Rev. Lett. **101**, 023601 (2008).
[4] K. K. Ni, S. Ospelkaus, D. Wang, G. Quéméner, B. Neyenhuis, M. H. G. de Miranda, J. L. Bohn, J. Ye, and D. S. Jin, Nature **464**, 1324 (2010).
[5] L. Scharfenberg, S. Y. T. van de Meerakker, and G. Meijer, PhysChemChemPhys **13**, 8448 (2011).
[6] L. Scharfenberg, K. B. Gubbels, M. Kirste, G. C. Groenenboom, A. van der Avoird, G. Meijer, and S. Y. T. van de Meerakker, Eur. Phys. J. D **65**, 189 (2011).
[7] R. V. Krems, PhysChemChemPhys **10**, 4079 (2008).
[8] A. Andre, D. Demille, J. M. Doyle, M. D. Lukin, S. E. Maxwell, P. Rabl, R. J. Schoelkopf, and P. Zoller, Nat. Phys. **2**, 636 (2006).
[9] H. J. Loesch and B. Scheel, Phys. Rev. Lett. **85**, 2709 (2000).
[10] M. Strebel, S. Spieler, F. Stienkemeier, and M. Mudrich, Phys. Rev. A **84**, 053430 (2011).
[11] S. A. Rangwala, T. Junglen, T. Rieger, P. W. H. Pinkse, and G. Rempe, Phys. Rev. A **67**, 043406 (2003).
[12] T. Rieger, T. Junglen, S. A. Rangwala, G. Rempe, P. W. H. Pinkse, and J. Bulthuis, Phys. Rev. A **73**, 061402 (2006).
[13] C. Sommer, M. Motsch, S. Chervenkov, L. D. van Buuren, M. Zeppenfeld, P. W. H. Pinkse, and G. Rempe, Phys. Rev. A **82**, 013410 (2010).
[14] B. Bertsche and A. Osterwalder, Phys. Rev. A **82**, 033418 (2010).
[15] B. Bertsche and A. Osterwalder, PhysChemChemPhys **13**, 18954 (2011).
[16] Y. Xia, L. Deng, and J. Yin, Appl. Phys. B **81**, 459 (2005).
[17] Y. Xia, Y. Yin, H. Chen, L. Deng, and J. Yin, Phys. Rev. Lett. **100**, 043003 (2008).
[18] L. Deng, Y. Liang, Z. Gu, S. Hou, S. Li, Y. Xia, and J. Yin, Phys. Rev. Lett. **106**, 140401 (2011).
[19] M. Sun and J. Yin, Phys. Rev. A **78**, 033426 (2008).
[20] J. van Veldhoven, H. L. Bethlem, M. Schnell, and G. Meijer, Phys. Rev. A **73**, 063408 (2006).
[21] R. L. Bhattacharjee, J. Mol. Spectrosc. **138**, 38 (1989).
[22] L. Deng and J. Yin, J. Opt. Soc. Am. B **27**, A88 (2010).
[23] C. E. Heiner, H. L. Bethlem, and G. Meijer, Chem. Phys. Lett. **473**, 1 (2009).
[24] S. A. Meek, H. Conrad, and G. Meijer, Science **324**, 1699 (2009).
[25] A. I. Gonzalez Florez, S. A. Meek, H. Haak, H. Conrad, G. Santambrogio, and G. Meijer, PhysChemChemPhys **13**, 18830 (2011).
[26] Y. Yin, T. Li, P. Xu, H. Jin, and S. Zhu, Appl. Phys. Lett. **98**, 093105 (2011).